

ADVANCED PROCESS DESIGN IN HIGH VOLUME KNEADER REACTORS USING MULTIPLE FEED PORTS TO AVOID CRUST FORMING, FOAMING AND LOW HEAT TRANSFER

Daniel U. Witte
LIST USA Incorporation
Charlotte, NC 28217-2809

Abstract

Kneaders reactors are used for combined unitary processing in the polymer industry for devolatilization, compounding or polymerization. Multiple feed ports are used in screw type reactors to allow adding multiple substrates into one product whereas one unitary operation has to get to a certain degree of completion before the next substrate can be added. We have found that even for identical substrates multiple feed ports can be advantageous to avoid specific working points, where the product behavior is disadvantageous for efficient processing. Such processes require advanced design simulation tools to predict process behavior. We compare simulation results on pilot and the scale up.

Introduction

Screw type reactors including kneaders are generally described as plug flow machines. Typically a high degree of mixing efficiency is desired. Therefore there is always some degree of axial dispersion associated with the desired radial and tangential dispersion (see Figure 1). The typical approach to account for this dispersion is to describe it by an axial dispersion model characterized by the Bodenstein number. The modeling of this is a common engineering practice in chemical engineering. As an example Trolstra [1] has applied this method to describe PMMA bulk polymerization in a Buss Co-kneader. The advantage of this approach is that the energy and mass balance can be described by using a differential term just like the plug flow model, and then numerically integrating over the reactor length. If additional feed ports are distributed over the length of the machine, the numerical method to account for them is to interrupt the integration and adjust the boundary conditions (the additional feed) and restart the integration again.

In high volume kneaders, mixing sections are typically identical over the length of the machine. These machines have a much higher hold up than extruders and co-

kneaders and the amount of axial dispersion is also greater due to higher hold up and consequently longer residence time in the machine. The different sections of the machine are open, which facilitates axial dispersion. We found previously that in high volume kneaders, it is possible to have backmixed sections in the machine. The proof that this is happening is that in evaporation you can start with a dry bed of viscous material or the diluted feed solution and find different steady state conditions. The axial dispersion model cannot predict conflicting working points dependent on the way the kneader was started up, whereas the model of continuous CSTR can. The goal of this study was to check if a model of tanks in series could efficiently predict these competing working points and use the model to find optimal working conditions allowing greatly increased production rates.

Experimental

The experimental set up is divided into sections:

1. The 1st part of the study was to describe the degree of backmixing for a specific machine length. The tank in series model predicts that if you double the machine length, the number of tank in series has to be doubled also to describe the backmixing effect. The kneader is fed by silicon mass and discharged under steady state conditions. Color is injected and the color response (concentration) is determined over time at the discharge. Thus we determined the E distribution function and fit the theoretical curve of a specific number of tanks in series through the experimental data.
2. Rubber cement solution was fed into a kneader evaporator. The feed port was at the front end of the kneader and the discharge at the opposite end. The rate and amount of solvent evaporated as well as the mechanical heat input by the agitator were monitored during the tests. We also measured the temperature profile over the length of the machine. Assuming the solution is boiling and therefore in equilibrium, the measured temperature corresponds to a solvent concentration in that section. Both parameters correspond to a cement viscosity, which allows

predicting the mechanical heat input [2]. We tried to match the temperature data points using different heat transfer coefficients.

3. The section 2 showed that indeed there are different conflicting working points that the model would predict. Evaporation was found higher at specific solvent concentrations and not necessarily at highest solvent concentrations. This suggests that a system using several feed ports would be beneficial. We tested the same system as described in section 2 using a 2nd feed port at some length of the kneader. In order to compute the results with the model, we calculated the amount of solvent we would have fed to each tank in series and compared the results with geometrical (actual) feed situation.

The different parts of the study are described in detail as follows:

Part 1: residence time distribution study

The equipment we tested is a model of a single shaft high volume kneader as shown on Figure 2. There are static elements, the counterhooks, mounted on the shell, which interact with dynamic elements mounted on the shaft, the bars welded on the discs and the T-fingers, which are directly welded to the shaft. These interactions provide self cleaning of the machine, but also the dispersion of the ink into the viscous mass. We used the silicon paste Baysilone 500.000 [3] as the continuous flow media through the machine. The feed was provided by means of a pressurized piston, which fed a Moyno pump to control the throughput (Figure 3). The piston and the kneader was standing on load cells allowing adjusting the kneader hold-up. A hydraulic motor drove the main shaft of the kneader. The housing of the kneader was made of Plexiglas, which allows observing what happens in the kneader and is also lightweight. This means that the weight determination of the hold up is more precise compared to a real kneader type machine, which has a casing and heating jacket in steel. The silicon paste was extracted from the kneader by means of a mono-screw.

After injection of the color, samples were taken manually and the sampling time noted. The color concentration was determined by liquid chromatography by Solvias in Basel (CH).

To determine the E function, you have to consider that the integral over time of E from 0 to indefinite is equal to 1. Therefore:

$$E(t) = \frac{\dot{m}_{ink}}{m_{ink,tot}} \quad (1)$$

Eq. 1 implies that the total throughput of silicon is identical to the total mass stream. This is close to correct since the amount of ink we injected is much smaller than the silicon throughput. During the trials, samples were

taken until no ink could be visually detected any more. Even though it is difficult to assess a specific ink concentration by visual observation, the visual low-level detection of ink works quite well. Still we found that there was discrepancy between the different runs that up to 20 % of the injected ink was not detected. While this fact can be attributed to a number of reasons (dead areas in the kneader, lack of precision of ink detection method etc.), we needed a practical method for how to correct the values. The E function is the differential of the Tromp curve. By numerically integrating E from 0 to the last data point, we find a corrective factor we can then apply on E:

$$E_{corr}(t) = \frac{E(t)}{\int_0^{t_{\omega}} E(t) dt} \quad (2)$$

The E-function has the dimension 1/s. The tank-in-series model is applicable for any residence time. The missing link to get a general expression from the E-function is the mean residence time. This is the time when 50 % of the ink has passed:

$$\int_0^{\tau} E_{corr}(t) dt - 0.5 = 0 \quad (3)$$

From the theory there are different methods to fit the tank and series model through the empirical E data. From the author's point of view the most useful fit is to exploit the data point at τ . Using a Gauss Square method leads to a lot of spreading of the results, since the E-function may have a time shift in some areas:

$$E_{corr}(\tau)\tau = \frac{N_{tk}^{N_{tk}} e^{-N_{tk}}}{\Gamma(N_{tk})} \quad (4)$$

Since the kneader is comprised of separating discs, it makes sense to have at least two injection points over the kneader length and determine the number of theoretical stirred tanks between the two injection points. By this means the residence time behavior of the discharge section, which is supposedly identical between the two injection points, has not to be considered:

$$N_{tk,\Delta l_s} = \frac{N_{tk}(l_1) - N_{tk}(l_2)\Delta l_s}{l_1 - l_2} \quad (5)$$

Part 2: Rubber evaporation

The principle of continuous main evaporation has been described in previous papers and is patented [4]. The original idea was that the kneader would be shortened in L over D so that the axial backmixing would be enhanced that we could simulate the kneader as a single CSTR. This would allow running the kneader with a highly viscous mass of polymer in the kneader, homogeneously distributed in the kneader, in which the fresh cement solution would be incorporated. The advantages of this approach is that with an intermediate cement concentration, the boiling generates a large amount of

foam, which is stable and does not move by Archimedes forces to the surface, where they would implode as they would for high solvent concentrations. This is due to the increased viscosity of the solution. The foam both inhibits heat transfer by insulating the clearances between the paddles of the kneaders and the heat transfer surfaces, and by limiting the level of vacuum pressure you can apply without the foam being dragged off into the off-gas vapor dome. At higher polymer concentrations, the viscosity is high enough to crush down that foam and also the generated friction helps to produce mechanical heat input to further accelerate the evaporation. The theoretical model is obvious in its benefits, however in reality the improved backmixing is limited to 2 to 3 disc rows as the results of part 1 of this study will show, hence this second part of the study. The evaporation in a CSTR is described as following:

$$\begin{aligned} \dot{Q}_{mech,i} + \alpha(w_i, T_i) A_i (T_W - T_i) + \dot{m}_{pol}(T_{i-1} - T_i) \left(c_{p,pol} + c_{p,liq} \frac{w_i}{1-w_i} \right) \\ = \Lambda h_v \dot{m}_{pol} \left(\frac{w_{i-1}}{1-w_{i-1}} - \frac{w_i}{1-w_i} \right) \end{aligned} \quad (5)$$

The kneader is divided into $N_{tk,L}$ sections and geometrical data for each section, as e.g. heat transfer area, is determined. The mechanical heat input is dependent on viscosity and fill in that section. The viscosity is a function of temperature, solvent concentration and shear rate (which links to shaft RPM). A proprietary model was used to link these parameters into a separate function [2]. The fill is estimated in the 1st vessel and the fill profile over length can then be calculated for the following vessels [5]. A loop calculation will approximate the measured mechanical heat input to the calculated one.

Eq. 5 is not sufficient to solve the heat and mass balance. Since we could not take samples over the kneader length, we assume that the boiling of the solution is in equilibrium. The equilibrium is described by the simplified Flory-Huggins interaction parameter (molecular mass of solvent much smaller than that of polymer):

$$\frac{p}{p_0(T_i)} = e^{\ln(X_{liq}) + 1 - X_{liq} + \chi(1 - X_{liq})^2} \quad (6)$$

This equation means that a single-phase vapor environment in the kneader can be assumed. The operating pressure p is uniform in the kneader since the gas section is interconnected. The volume concentration of liquid in the cement solution has to be determined from the mass concentration using the respective densities of liquid and polymer.

In order to determine the equilibrium data, we chose to do a semi-batch test upfront of the continuous testing. The semi-batch test set up is shown on Figure 4. The feed solution was fed from a pressurized tank. The pressure in this tank was kept constant by a pressure reducer releasing N_2 into tank to replace the subtracted cement solution. This solution was a mixture of different BR rubber grades and

different solvents, with hexane the most prominent. The cement solution feed into the kneader was controlled by a flow metering valve and the flow determined by a Coriolis mass flow meter. The kneader was equipped with a pressure transducer to control and monitor the vacuum pressure in the vessel. The vapors were relieved from the vessel by a vapor dome, compressed and condensed. Load cells under the receiving pot monitored the amount of condensed solvent.

The kneader was equipped with 3 RTDs mounted in the counterhooks of the vessel and with a hydraulic motor to drive the main shaft. The hydraulic pressure was measured using a transducer. The shaft torque is proportional to the net hydraulic pressure difference. This pressure was measured while the kneader was still empty for different shaft speeds. During the test with product, we subtracted this empty load pressure from the measured pressure to obtain the net hydraulic pressure difference. The shaft speed was monitored using a proximity switch. The mechanical heat input can then be determined easily:

$$\sum_{i=1}^{N_{tk,L}} \dot{Q}_{mech,i} = 2\pi n_S T_S \quad (7)$$

During the semi-batch trial, we tried to keep the fill in the kneader fairly constant at around 40 %. This is done by visual check through a sight glass on top of the kneader. The cement solution was dried as much as possible. Then we switched over to continuous processing. It is advantageous to use the same equipment for the batch and the continuous process since we can monitor the torque characteristic of the product as well (which will depend on the kneader geometry).

The continuous set up (see Figure 4) was similar to the semi batch, but a twin screw discharged the material. This screw fed into a gear pump, which sent the material to a finisher for further devolatilization.

Part 3: 2nd feed port

For this part of the study we added a 2nd feed port into the vapor section further down the length of the kneader to the experimental set up (see Figure 4). This feed port had its dedicated Coriolis mass flow meter.

The extrapolation of the results was much different from the second part of this study. During operation, we were trying to match a certain temperature profile by increasing or reducing feed from the particular feed port. That means the feed distribution is now a potential control parameter, whereas with one feed port it is not. The simulation is therefore done by calculating the solvent concentration profile using eq. 6 and then resolving eq. 5, where the additional contribution (enthalpy) of the feed port of chamber i has been added. Again, the initial fill of chamber 1 is estimated, but the axial conveying has been integrated into the calculation, because the additional feed ports may influence the conveying. The sum of all

calculated feed streams has to match the amount of feed solution during the test. We can then interpolate either over the initial fill of the machine to match this criterion, or choose the shaft speed as the free parameter.

Results and discussion

Part 1: residence time distribution study

Table 1 shows the RTD analysis. The use of the Gamma function (see eq. 4) allows determining numbers of stirred tanks in series, which are in between natural numbers. Our model though cannot use these not natural numbers. We therefore chose 1 as the best fit to all the runs. The data suggests that different working conditions (shaft speed, transport angle) have surprisingly little impact on the number of determined stirred tanks per disk row.

A big problem of this part of the study was the sampling and the analytical part. We took about 20 samples per run and there was a total of 21 runs. Additional 30 reference samples were prepared to calibrate the analysis. The ink tended to settle requiring each sample to be stirred before analysis. Since we tested only one type of fluid, we could ask ourselves if lower viscosity material would not mix better and quicker.

Part 2: Rubber evaporation

As mentioned before, the study started with the assumption that a 100 % backmixed CSTR could be achieved. The 1st part of the study revealed that our test machine, which had 4 disc rows would perform rather as 4 CSTR in series. Figure 5 shows an example of temperature profile over the kneader length direction. We can see that there is an increase towards the discharge, which could not be explained with one single stirred tank.

Now the goal was to find out whether the machine made of 4 stirred tanks would perform as well as a single tank would. We ran the evaporator at 15 kg per hr feed solution and 40 RPM shaft speed at continuous steady state. Then we gradually increased the feed rate to 20 kg per hr. We then found the temperature profile became more and more stiff and that we had to cool the material towards the discharge of the kneader more and more to keep the polymer from overheating at the discharge end. At maximal throughput, the process became unstable and the machine flooded with liquid cement solution. The process only returned to its original working point by drastically cutting the feed rate and then slowly regaining the original feed rate again.

Figure 6 shows the process simulation of one of the stirred tanks. The criterion that is plotted against the solvent concentration is the combined mass and heat balance. This criterion has to match 0. The solution curve has a cubic type shape. The left side is the heat transfer controlled area. For the first vessels, the solution is dilute

and this regime is predominant. With decreasing solvent concentration, the viscosity increases and the mechanical heat contribution becomes greater. This means that the curve shown on Figure 6 essentially moves down with increasing vessel number i . The interesting part is when the two regimes compete against each other. There are up to three different solutions, which can be found, thus three possible outlet concentrations and temperatures, which solely differ with regards to the history preceding the steady state conditions. This finding is significant because it explains why the process run had not been stable. This is also a numerical problem, since the process engineer does not know which of the solutions the simulation program will converge. Further scale up work revealed that for higher number of stirred tanks (above 5), the performance of the evaporator would be similar to a plug flow evaporator, at 3 the process would be unstable and only stable again below 2. This means that this process solution would be at a dead end if we could not further improve the backmixing behavior of the evaporator.

Part 3: 2nd feed port

Figure 7 shows the evaporation rate for different evaporator shaft speed that we ran. The 2nd feed port was highly beneficial since we were able to double the throughput rate compared to one feed port. The machine torque was kept constant for all runs. Figure 9 shows the large input of mechanical heat input. This corresponds to the original goal to dissipate the evaporation energy through mechanical shear into a viscous mass of polymer.

Table 2 shows the simulated feed distribution compared to the actual feed situation. We see that there are some discrepancies, but we can explain it because the feed solution has to find its way into the polymer solution. This means the amount of feed that goes in one or the other chamber is not only dependent on where the feed is positioned, but also in regards to where the agitator elements are. The preferred feed position is the tip of the disc.

The simulation also revealed that we can run the evaporator not only with viscous material to achieve optimal performance, but that at solvent concentrations around 40 % the heat transfer is potentially also very good. In this area the solution is viscous enough to crush down the foam, but not viscous enough to introduce much mechanical shear. Still the heat transfer coefficient is in the order of 300 to 500 W/m²/K compared to 10 to 30 W/m²/K when there is foam present in kneader clearances, while the cement temperature is still low enough to provide sufficient driving force.

Summary

A new method of processing using multiple feed ports in high volume kneaders has been developed. A process simulation tool has been developed to predict performance in a polymer cement evaporator. The new process provides new opportunities to process more efficiently and to avoid non-efficient working points by backmixing. Thus we were able to develop an evaporator, which works more consistently and at much greater throughput rates together with a method how to scale up the process to industrial size.

Nomenclature

A	heat transfer surface
c	concentration
c_p	specific heat
E(t)	Residence time distribution (E function)
l_i	distance feed side to injection port i
m	mass
\dot{m}	mass flow
N	number
n_s	shaft speed
p	operating pressure
p_0	vapor pressure
$\dot{Q}_{mech,i}$	mechanically dissipated power into chamber i
t	time
T_s	shaft torque
T	temperature
w	solvent content
X	volume fraction

greek:

α	heat transfer coefficient
Γ	Gamma function
Δl_s	distance between 2 discs
Δh_v	heat of evaporation of solvent
τ	mean residence time
χ	Flory-Huggins interaction parameter

indices:

corr	corrected
ink	of ink
L	kneader process chamber length
pol	polymer
liq	liquid (solvent)
S	shaft
silicon	of silicon
tk	of theoretical stirred tanks in series
tot	total

W	wall (jacket or shaft)
ω	end of sampling

References

1. Erik Troelstra, The Buss-Kneader as Polymerization Reactor for Acrylates, PhD thesis at Rijksuniversiteit Groningen, 1998
2. Diploma work D. Jermann/T. Lukic "Newton-Reynoldszahl für LIST-Kneter", Fachhochschule beider Basel (FHBB), 2003
3. Manufactured by GE Bayer
4. European patent EP1127609
5. Daniel Witte, Axial Transport in Kneader Reactors, Antec (2007)

Key Words

Multiple, feed port, evaporation, kneader, simulation, tank-in-series

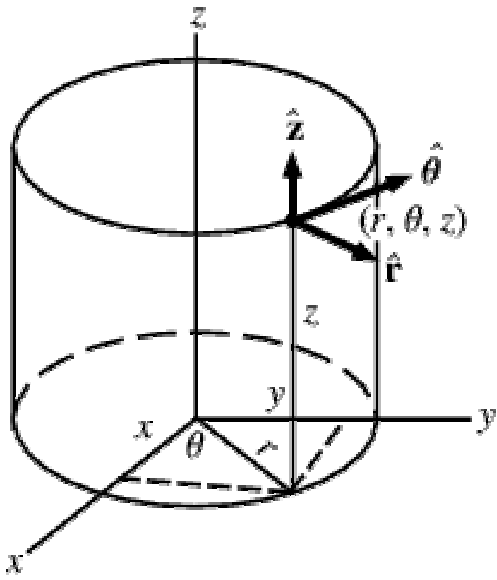


Figure 1: Cylindrical coordinates, z would be the main transport direction, which is horizontal in kneaders and extruders. The radial direction is described by r and the tangential direction by θ

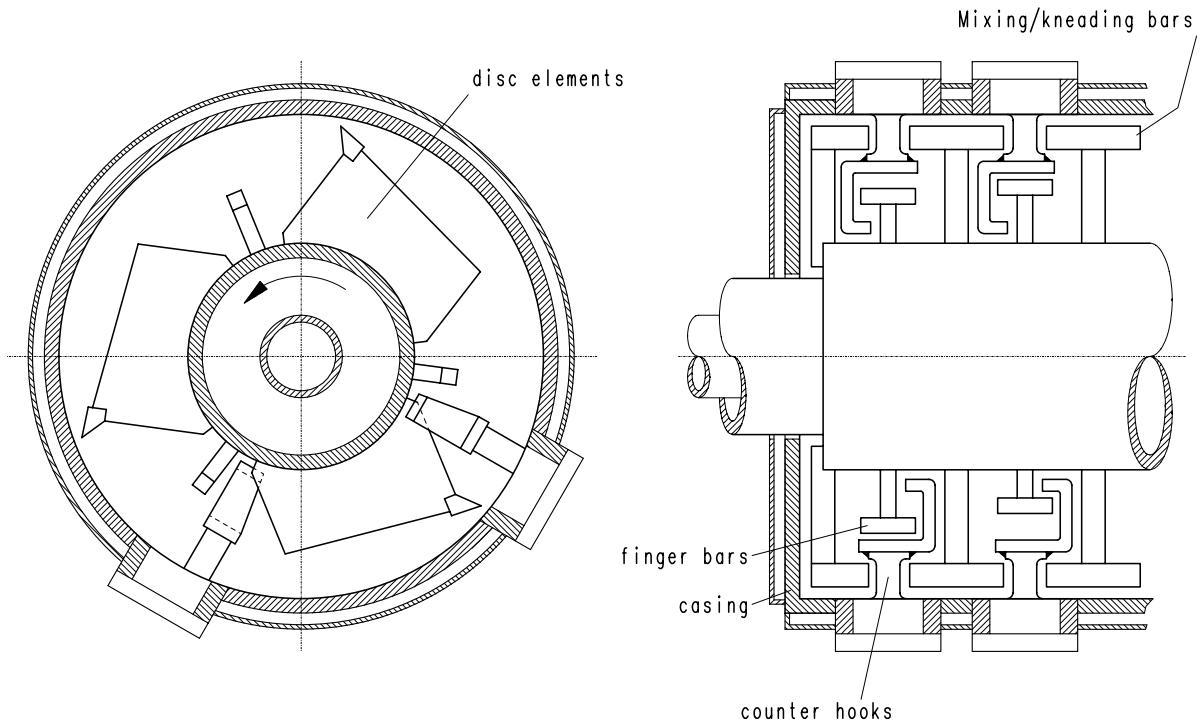


Figure 2: Single shaft kneader



Figure 3: Test set up for silicon color injection trials

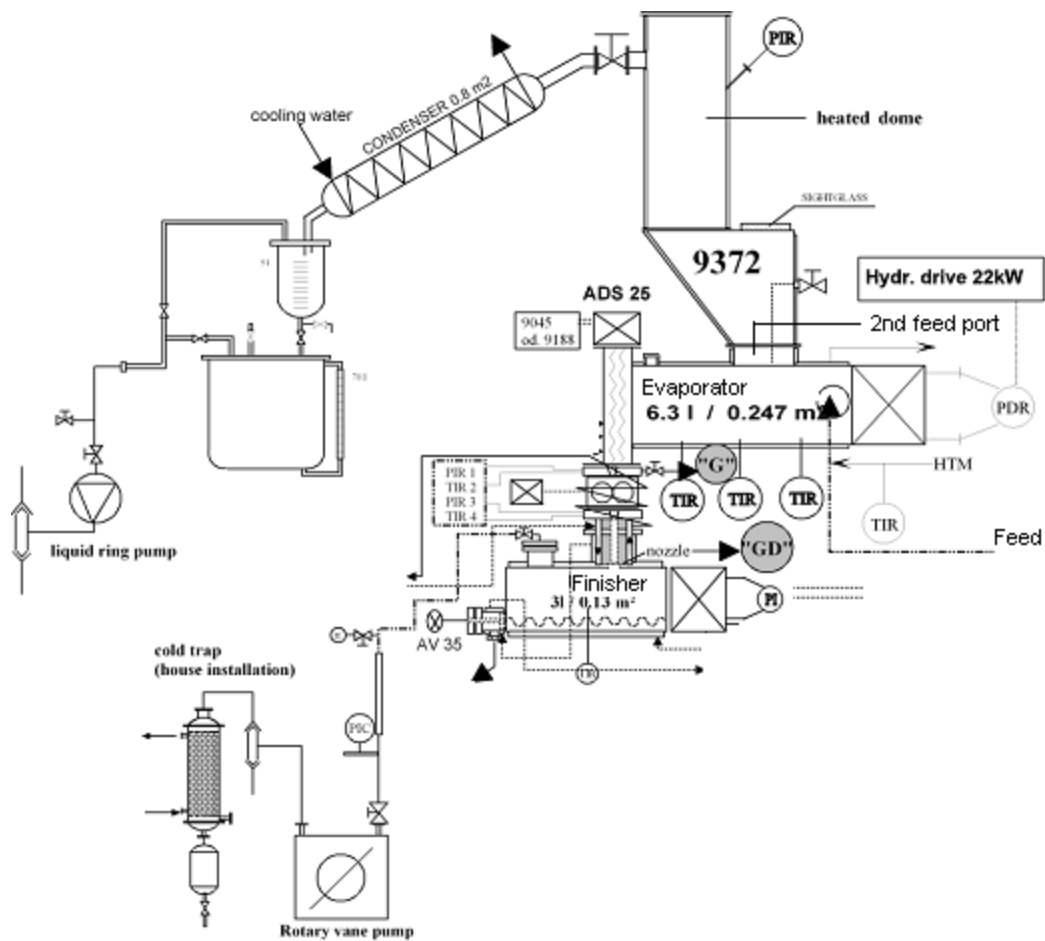


Figure 4: Test set up for evaporation trial

run 1	1.021
run 2	1.653
run 3	1.78
run 4	1.581
run 5	1.915
run 6	1.006
run 7	1.106
run 8	0.803

Table 1: Results of RTD (number of stirred tanks) on one disc length for various working conditions on a 6 l kneader

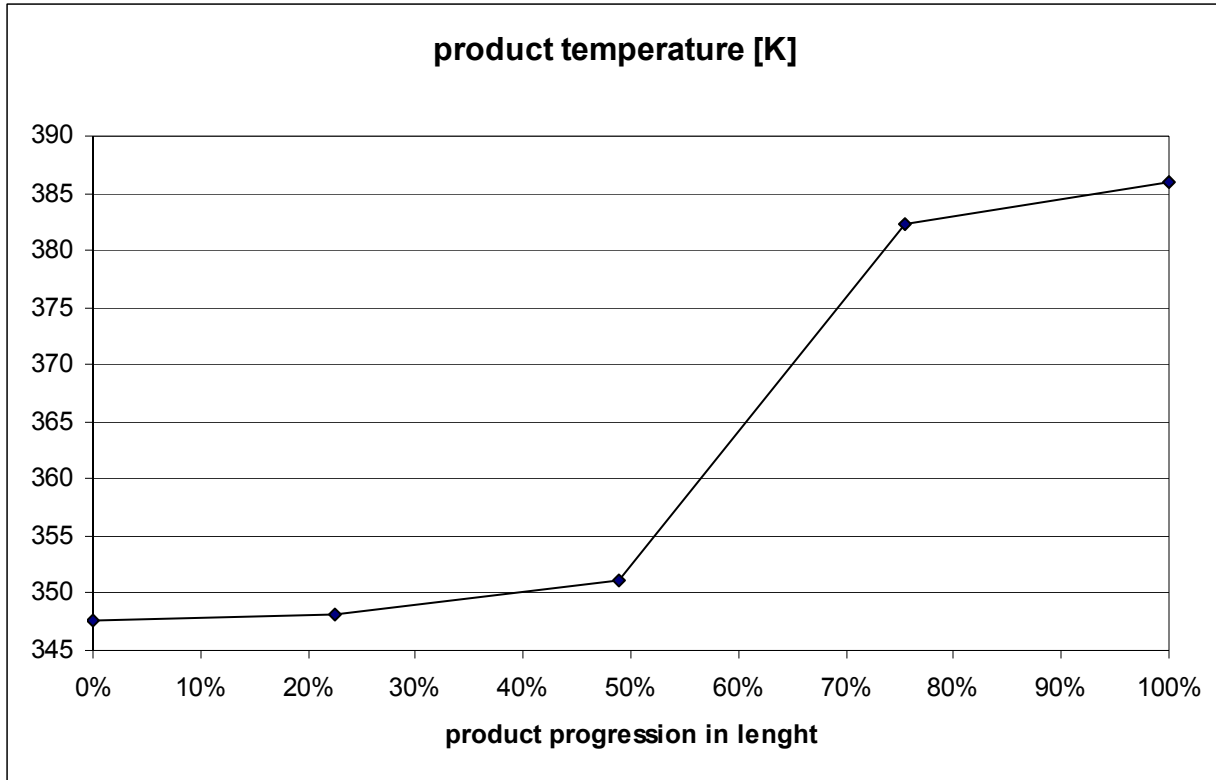


Figure 5: Temperature profile in kneader evaporator

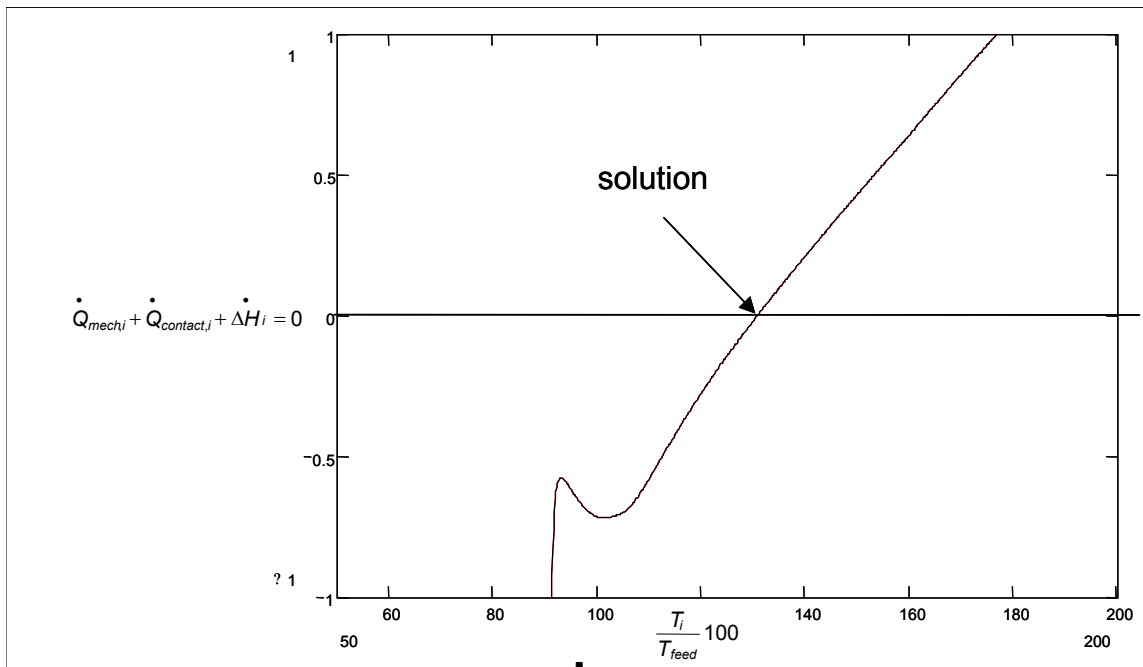


Figure 6: Heat and mass balance criterion over product temperature of vessel I

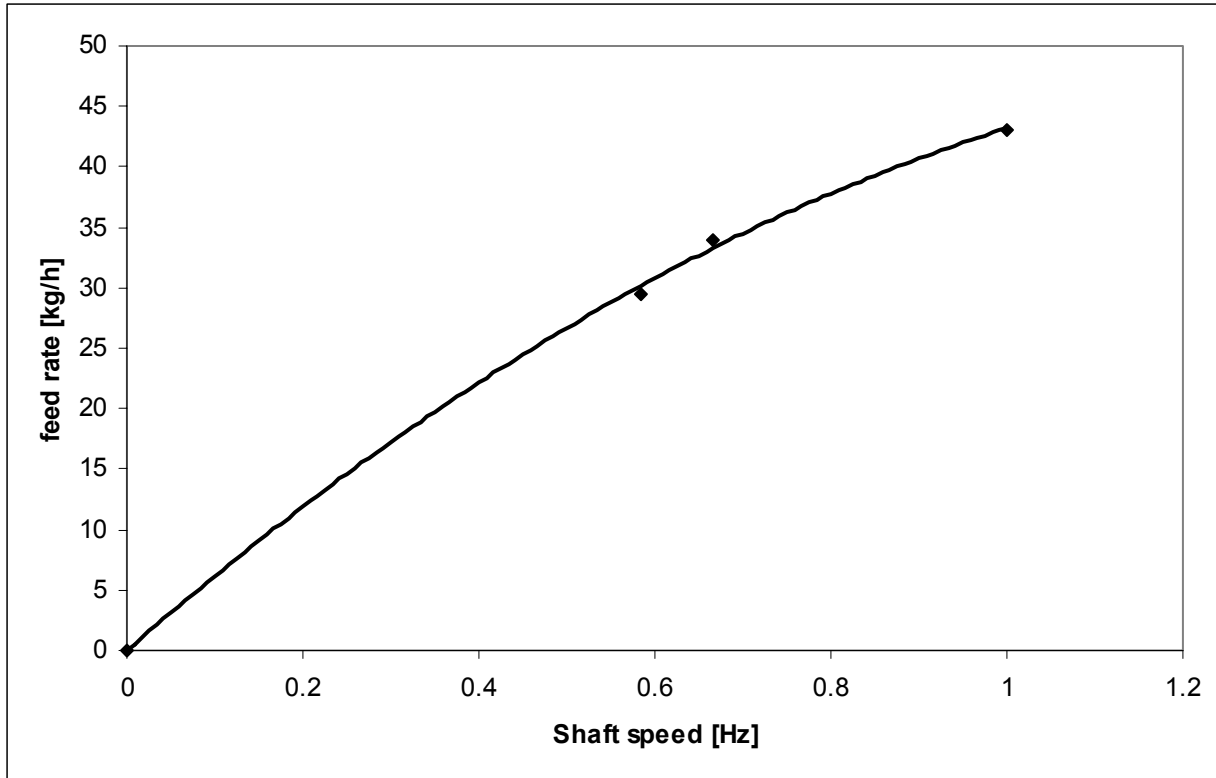


Figure 7: Cement feed rate versus kneader main shaft speed

Shaft speed [Hz]	Feed rate [kg/h]	Chamber #	Fraction of feed rate (geometrical)	Fraction of feed rate (simulated)
0.68	23	1	0.671	0.739
		2	0.329	0.258
		3	0.000	0.070
		4	0.000	-0.067
0.67	32	1	0.336	0.534
		2	0.486	0.386
		3	0.178	0.175
		4	0.000	-0.095
1.00	41	1	0.336	0.458
		2	0.486	0.545
		3	0.178	-0.007
		4	0.000	0.004

Table 2: Comparison actual and simulated feed distribution